Molecular cloning and functional expression of $Ca_v3.1c$, a T-type calcium channel from human brain

Leanne L. Cribbs, Juan Carlos Gomora[1], Asif N. Daud, Jung-Ha Lee[1], Edward Perez-Reyes[1,*]

Department of Physiology and the Cardiovascular Institute, Loyola University Medical Center, Maywood, IL 60153, USA

Received 3 December 1999

Edited by Maurice Montal

Abstract Low voltage-activated T-type calcium channels are encoded by a family of at least three genes, with additional diversity created by alternative splicing. This study describes the cloning of the human brain α1G, which is a novel isoform, $Ca_v3.1c$. Comparison of this sequence to genomic sequences deposited in the GenBank allowed us to identify the intron/exon boundaries of the human CACNA1G gene. A full-length cDNA was constructed, then used to generate a stably-transfected mammalian cell line. The resulting currents were analyzed for their voltage- and time-dependent properties. These properties identify this gene as encoding a T-type Ca^{2+} channel.

Key words: Calcium channel; Molecular cloning

1. Introduction

Voltage-gated calcium channels are formed by large α1 subunits that contain the voltage sensing and pore forming regions. Ten α1 genes have been cloned [1]. Based on similarities in their deduced amino acid sequences, these α1 subunits can be classified as belonging to one of three groups: Ca_v1, or L-type family, is composed of α1S, α1C, α1D and α1F; the Ca_v2 family is composed of α1A, α1B and α1E; and the Ca_v3 or T-type family (Ca_vT), is composed of α1G, α1H and α1I [1]. These channels play a central role in modulating intracellular calcium concentrations, and hence control muscle contractility, gene expression, and secretion of neurotransmitters and hormones [2].

In this study, we cloned a novel splice variant of the human α1G gene, CACNA1G, which we call $Ca_v3.1c$. The full-length cDNA was transfected into human embryonic kidney cells (HEK-293), and a stably-transfected cell line was isolated. The basic electrophysiological properties of the resulting T currents were characterized. We then took advantage of the well-isolated currents to study the dose-dependent block of T-type channels by nickel.

2. Materials and methods

2.1. Cloning of human α1G

The full-length α1G cDNA was cloned by multiple screens of cDNA libraries (Clontech, Palo Alto, CA, USA) from either human thalamus or cerebellum. Screening was done by filter hybridization according to the manufacturer's protocol. The cDNA probes were synthesized using [α-^{32}P]dCTP and a labeling kit (Amersham Pharmacia Biotech, Piscataway, NJ, USA). The full-length cDNA (hα1G) was assembled from the overlapping cDNA fragments shown schematically in Fig. 1A. The 'hgfinPCR' fragment was synthesized by RNA-PCR using human brain mRNA (Clontech) and the following PCR primers: forward, 5′-G-A-C-A-A-C-A-T-C-G-G-C-T-A-C-G-C-C-T-G-G-A-T-C-3′; reverse, 5′-G-G-G-G-G-G-C-C-C-C-G-G-A-G-A-G-G-G-C-A-G-G-3′. This resulted in 'hgfinPCR' (1012–1638). The 5′ clone 'Fre12u' (−216–1342) was ligated to the *Sal*I site of 'hgfinPCR'. This was connected to clone 'C5' (cerebellum, 1473–2695) at the *Sfi*I site, then to clone 'C7' (cerebellum, 2360–3713) at the *Nsi*I site, then to the 3′ clone '15-2' (thalamus, 3400–7187) at the *Xho*I site. The fully-assembled cDNA (−216–6949) was then cloned into the *Kpn*I site of the transfection vector pcDNA3 (Invitrogen). The full-length cDNA was sequenced on both strands.

2.2. Electrophysiological analysis of HEK-293 transfected cells

Preparation of a stably-transfected cell line expressing the rat α1G ($Ca_v3.1a$) was described previously [3]. Similar methods were used to generate a cell line expressing the human α1G 'hα1G-39'. The methods used to prepare the cells for electrophysiological studies have been described previously [3]. The recording solution contained the following (in mM): 10 $BaCl_2$, 155 tetraethylammonium chloride, 6 CsCl, and 10 HEPES, pH adjusted to 7.4 with tetraethylammonium hydroxide. The standard internal pipette solution contained the following (in mM): 65 CsCl, 75 $CsMeSO_4$, 1 $MgCl_2$, 4 MgATP, 1 EGTA, and 10 HEPES, pH adjusted to 7.3 with CsOH.

Whole-cell currents were recorded from ruptured patches using an Axopatch 200B amplifier, Digidata 1200 A/D converter, and pCLAMP 7.0 software (Axon Instruments, Foster City, CA, USA). Data were filtered at 5 kHz and digitized at 10 kHz, except for tail current measurements, which were digitized at 50 kHz. Pipettes were made from TW-150-6 capillary tubing. The pipette resistance was typically 1.5–2.0 MΩ. Series resistances and cell capacitance were compensated at least 80%. The average cell capacitance was ~25 pF. All experiments were performed at room temperature with constant perfusion of the bath (1–3 ml/min). Leak currents were minimal, therefore online leak subtraction was not used. A 100 mM $NiCl_2$ stock solution was prepared in deionized water. Peak currents and exponential fits to currents were determined using Clampfit software (Axon Instruments). Fits and graphs of the data were done with Prism (GraphPad, San Diego, CA, USA). Average data are presented as mean ± S.E.M.

3. Results

Cloning of the T-type Ca^{2+} channel family began with the identification of a human EST clone as belonging to a novel ion channel [4]. Due to the difficulties in cloning an 8.5 kb cDNA from a single library and in obtaining undegraded

*Corresponding author. Fax: (1)-804-982 3878.
E-mail: eperez@virginia.edu

[1] Present address: Department of Pharmacology, Box 448, Jordan Hall, University of Virginia, Charlottesville, VA 22908, USA.

PII: S0014-5793(99)01756-1

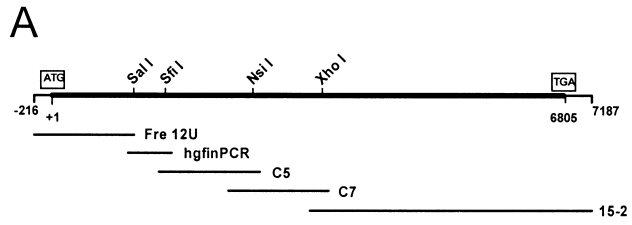

B

```
MDEEEDGAGA EESGQPRSFm rLNDLSGAGG RpGPGSaEKD PGSADSEAEG LPYPALAPVV
FFYLSQDSRP RSWCLRTVCN PWFERiSMLV ILLNCVTLGM FRPCEDIACD SQRCRILQAF
DDFIFAFFAV EMVVKMVALG IFGKKCYLGD TWNRLDFFIV IAGMLEYSLD LQNVSFSAVR
TVRVLRPLRA INRVPSMRIL VTLLLDTLPM LGNVLLLCFF VFFIFGIVGV QLWAGLLRNR
CFLPENFSLP LSVDLErYYQ TENEDESPFI CSQPRENGMR SCRSVPTLRG dGGGGPPCgL
DYEaYNSSSN TTCVNWNQYY TNCSAGEHNP FKGAINFDNI GYAWIAIFQV ITLEGWVDIM
YFVMDAHSFY NFIYFILLII VGSFFMINLC LVVIATQFSE TKQRESQLMR EQRVRFLSNA
STLASFSEPG SCYEELLKYL VYILRKAARR LAQVSRAaGV RvGLLSSPap lgGQEtQPSs
SCsRSHRRLS VHHLVHHHHH HHHHYHLGNG TLRaPRASPE IQDRDANGSR RLMLPPPSTP
alSGaPPgGA ESVHSFYHAD CHLEPVRCQA PPPRsPSEAS GRTVGSGKVY PTVHTSPPPE
tLKeKALVEV AaSsGPPTLT SlNIPPGPyS SMHKLLETQS TGACqSSCKI SSPClKADSG
ACGPDSCPYC ARaGAGEvEl ADreMPDSDS EAVYEFTQDA QHSDLRDPHS RRQRSLGPDA
EPSSVLAFWR LICDTFRKIV DSKYFGRGIM IAILVNTLSM GIEYHEQPEE LTNALEISNI
VFTSLFALEM LLKLLVYGPF GYIKNPYNIF DGVIVVISVW EIVGQQGGGL SVLRTFRLMR
VLKLVRFLPA LQRQLVVLMK TMDNVATFCM LLMLFIFIFS ILGMHLFGCK FASERDGDTL
PDRKNFDSLL WAIVTVFQIL TQEDWNKVLY NGMASTSSWA ALYFIALMTF GNYVLFNLLV

AILVEGFQAE GDAnKSESEP DFFSPSlDGD GDRKKcLALV sLGEHpELRK SLLPPLIIHT
AATPMSlPKS tSTGlGEALG paSRRTSSSG SAEPGAAHEM KsPPSARSSP HSPWSAASSW
TSRRSSRNSL GRAPSLKRRS PSGERRSLLS GEGQESQDEE ESSEEeRASP AGSDHRHRGS
LEREAKSSFD LPDTLQVPGL HRTASGRgSA SEHQDCNGKS ASGRLARaLR pDDPpLDGDD
adDEGNLSKG ERvrAWiRaR LPACClERDS WSAYIFPPQS RFRLLCHRII THKMFDHVVL
VIIFLNCITI AMERPKIDPH SAERIFLTLS NYIFTAVFLA EMTVKVVALG WCFGEQAYLR
SSWNVLDGLL VLISVIDILV SMVSDSGTKI LGMLRVLRLL RTLRPLRVIS RAQGLKLVVE
TLMSSLKPIG NIVVICCAFF IIFGILGVQL FKGKFFVCQG EDTRNITNKS DCAEASYRWV
RHKYNFDNLG QALMSLFVLA SKDGWVDIMY DGLDAVGVDQ QPIMNHNPWM LLYFISFLLI
VAFFVLNMFV GVVVENFHKC RQHQEEEEAR RREEKRLRRL EKKRRSKEKQ MA***DLMLDDVI***
***ASGSSASAAS*** EAQCKPYYSD YSRFRLLVHH LCTSHYLDLF ITGVIGLNVV TMAMEHYQQP
QILDEALKIC NYIFTVIFVl ESVFKLVAFg FRRFFQDRWN QLDLAIVLLS IMGITLEEIE
VNaSLPINPT IIRIMRVLRI ARVLKLLKMA VGMRALLdTV MQALPQVGNL GLLFMLLFFI
FAALGVELFG DLECDETHPC EGLGRHATFR NFGMAFLTLF RVSTGDNWNG IMKDtlRDCD
QESTCYNTVI SPIYFVSFVL TAQFVLVNVV IAVLMKHLEE SNKEAKEEAE LEAELELEMK
TLSPQPHSPL GSPFLWPGVE GpdSpDSPKP GAlHpaAHar sAShFSLEHP TMqPHPtElP
gPDLLTVRKS GVSRTHSLPN DSYMCRHGST AEgpLGHRGW GLPKAQSGSv LSVHSQPADT
SyILQLPKDa phLLQPHsAP TWGtIPKLPP PGRSPLAQRP LRRQAAIRTD SLDVQGLGSR
EDLLaEVSGP SpPLaRaySF WGqSStQaQQ hSrshSKiSK HmtpPAPCPG pEPnWgKgPP
ETRSSLELDT ELSWISGDLL pPggQEEPps PRDLKKCYSV EaQSCqRRPt sWLDEQRRHS
IAVSCLDSGS QPhLgtdPSn LGGQPLGGPG SRPKKKLSPP SItIDPPESQ GpRtPpSPGi
CLRRRAPsSD SKDPlaSgPp DSmAASPSPK KDvLSLSGLS SDPaDlDP
```

Fig. 1. Deduced amino acid sequence of human brain $Ca_v3.1c$. A: Schematic diagram of the human $Ca_v3.1c$ cDNA. A full-length cDNA was constructed from the five fragments using the indicated restriction enzyme sites. B: The deduced amino acid sequence of the human $Ca_v3.1c$ was compared to the rat $Ca_v3.1a$ [4], and amino acid differences are shown in lower case letters. Transmembrane regions and exon boundaries (♦) are marked above the sequence. Splice variation leads to the appearance of either 23 amino acids in the II-III loop, or 18 amino acids in the III-IV interdomain loop (bold italics).

human RNA, we first cloned the rat α1G. We now report the cloning of human α1G cDNAs and construction of a full-length cDNA from five overlapping clones (Fig. 1A). The sequence contains an open reading frame that would encode a 251 kDa protein composed of 2296 amino acids (GenBank No. AF190860). This deduced amino acid sequence is 93% identical to the rat and mouse α1G sequences (GenBank Nos. AF027984, AJ012569, respectively), with most substitutions occurring in the carboxyl-terminus. In contrast, the human α1G is only ~60% identical to either the human α1H or α1I sequences (GenBank Nos. AF073931, AF129133, respectively). The regions of highest identity are the putative membrane spanning regions, where the three human genes are approximately 90% identical.

Preliminary reports have described the existence of splice variants for the CACNA1G gene occurring in two locations, one immediately after the sixth transmembrane region of the second repeat, IIS6 [5], and the second in the middle of the III-IV linker [5,6]. The human genomic sequence (GenBank No. AC005921) was sequenced by the MIT Center for Genome Research (Birren, B., Linton, L., Nusbaum, C. and Lander, E., unpublished). Comparison of the cloned cDNAs to this genomic sequence allowed the determination of the intron/exon boundaries (Fig. 1B) and resolution of the mechanisms of alternative splicing. Splicing of the III-IV linker is the result of two processes. One, an alternative 3′ splice donor site is used at the end of an exon leading the presence or absence of seven amino acids (SKEKQMA). Two, this exon is either joined to a small exon encoding 18 amino acids (DLMLDDVIASGSSASAAS) or not. The combination of these two events produces four gene products. We propose a nomenclature where the original rat clone is called $Ca_v3.1a$, which contains the first but not the second sequence (+,−). A sequence lacking both regions is called $Ca_v3.1b$ (−,−; e.g. GenBank No. AF126965). The present sequence contains both regions ($Ca_v3.1c$). A sequence lacking the first, but containing the second region is called $Ca_v3.1d$ (e.g. GenBank No. AF125161).

The diversity after IIS6 is caused by insertion (GenBank No. AB012043) or skipping (present results) of a small exon that encodes 23 amino acids. Apparently similar splicing occurs in the rodent α1G genes [5,7]. Neither the functional significance of this splicing event, nor the correlation with the III-IV linker variations, has been reported. Two cDNAs for this region were cloned from the cerebellar library (C4 and C7), and neither contained this insert.

Functional expression of human $Ca_v3.1c$ was studied in a stably-transfected HEK-293 cell line. Fig. 2A shows a family of Ba^{2+} currents elicited by depolarizations in 10 mV increments from a holding potential of −90 mV. The characteristics of the generated current are similar to native T currents studied in isolation. Activation and inactivation kinetics are faster at more depolarized voltages, producing the typical pattern of criss-crossing traces observed in most recordings of native T-type Ca^{2+} currents [8–10]. The peak current in each episode was measured, averaged, then plotted as a function of the test potential to derive the current-voltage (*I-V*) relationship (Fig. 2B). Current started to be detectable at −60 mV, peaked near −20 mV, and reversed at a membrane potential around +50 mV.

There are several procedures to measure the activation of T-type Ca^{2+} channels, each with its limitations. In this study,

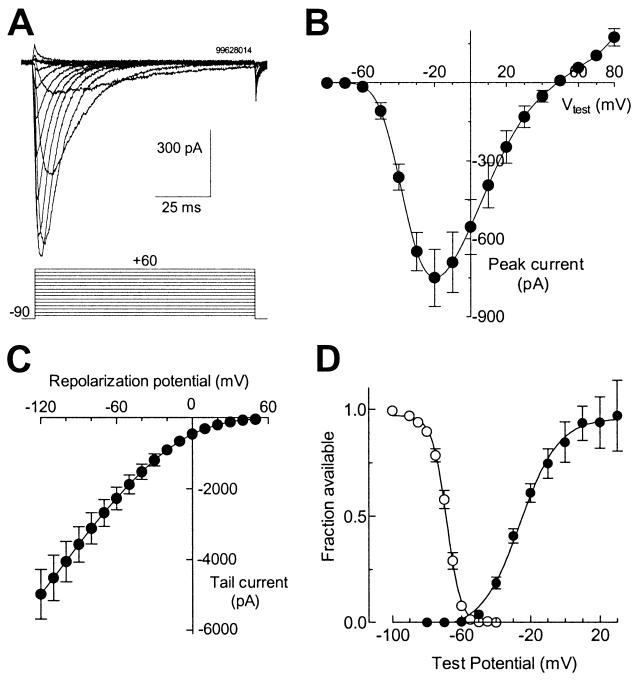

Fig. 2. Current-voltage (*I-V*) relation for human $Ca_v3.1c$ channels. A: Representative whole-cell Ba^{2+} currents obtained from a stably-transfected HEK-293 cell at 10 s intervals in response to 100 ms depolarizing pulses of 10 mV steps from a holding potential of −90 mV. B: *I-V* relationships averaged from 13 cells. Data points (mean ± S.E.M.) show peak current at each potential. C: Instantaneous *I-V* relation was measured using tail currents. Channels were activated by a 2 ms depolarizing pulse to +60 mV, and the amplitude of the tail current was measured after repolarization to different potentials. Recordings were filtered at 5 kHz and digitally sampled every 20 μs. Averaged tail current amplitudes ($n=7$) are plotted vs. repolarization potential. Currents were measured at the peak of the tail current, which varied from 0.35 to 0.55 ms. D: Activation curve was obtained by the following ratio: the peak current recorded using the *I-V* protocol (B) was divided by the instantaneous current recorded during repolarization from a 2 ms step to +60 mV (C). Experimental data points (●, $n=7$) were fitted with a Boltzmann function (smooth curve): $I=I_{max}/(1+\exp[-(V-V_{50})/k])$, where I is the peak current, I_{max} is the saturating value of I at positive membrane potentials, V_{50} is the voltage where one half of the channels are in the open conformation, and k is the slope factor (mV). Also shown is the voltage-dependence of steady-state inactivation. Human $Ca_v3.1c$ currents were activated by voltage steps to −20 mV after 30 s conditioning pulses to potentials between −90 and −40 mV. Data points (○, $n=11$) were fitted with a Boltzmann function (smooth curve). Inset: representative currents at −20 mV.

we used the method described by Serrano et al. [11] where the *I-V* data are divided by the instantaneous *I-V*. The protocol for obtaining the instantaneous *I-V* relationship included a short 2 ms pulse to +60 mV (to activate all the available channels and to minimize the inactivation), followed by a test pulse to different voltages ranging from −120 to +50 mV (inset, Fig. 3B). Because the same number of channels is expected to open during the +60 mV pulse, the only variable during the test pulses is the voltage-dependence of current flow through the open channel. The result shows a non-linear *I-V* relationship (Fig. 2C), suggesting complex interactions between permeant ions and the pore of the channel. The voltage-dependence of the activation of human α1G channels was finally obtained by dividing the *I-V* curve (Fig. 2B) by the instantaneous *I-V* curve (Fig. 2C). The result is shown in Fig. 2D. Each point of this curve is proportional to the number of channels open at the time of peak current at the respective voltage. Experimental data were fitted with a single Boltzmann function. The half-maximal activation for human α1G was reached at −26 mV, with a slope factor of 10.3.

The activation and inactivation kinetics of the human $Ca_v3.1c$ channels were studied using 100 ms pulses to different potentials. The current recordings were fitted with two exponentials and the results are shown in Fig. 3A. The rapid activation of the α1G channels was strongly voltage-dependent, with time constants ranging from 5.8 ± 0.8 to 0.9 ± 0.1 ms for membrane potentials between −50 and 0 mV ($n=16$). At more depolarized potentials (+10 to +40 mV), the current activates with a stable time constant around 0.9 ms. Current decay, or inactivation, was relatively slow at more negative voltages (−50 to −20 mV, $\tau=52.0\pm6.3$ and 10.7 ± 1.0 ms, respectively) and varied very little at voltages between −10 to +40 mV (9.8 ± 0.8 at +10 mV to 12.3 ± 1.8 at +40 mV).

We also studied the time course of deactivation produced by the closing of human $Ca_v3.1c$ channels after a short depolarizing pulse. The tail currents recorded with this protocol (Fig. 3B inset) were fitted with a single exponential and the time constants obtained are plotted in Fig. 3B. At very negative potentials, the closing of the channels was very sensitive to voltage changes. The time constant changed exponentially with voltage (*e*-fold for 33.8 ± 1.9 mV, $n=8$) for repolarization potentials between −120 and −50 mV. However, tail currents generated by repolarizations more positive than −50 mV showed little change in the time constant (from 8.1 ± 0.2 at −40 mV to 10.1 ± 0.9 at +40 mV). This result suggests that human α1G channel closing is voltage-dependent predominantly at extreme negative voltages.

The steady-state inactivation of human $Ca_v3.1c$ channels was studied by applying 30 s prepulses before a test potential to −20 mV to measure channel availability. The results are plotted in Fig. 2D and the inset shows representative current traces. The averaged data were fitted with a Boltzmann function with the following values: $V_{50}=-68.9$ mV and $k=4.6$. Similar results were obtained with rat $Ca_v3.1a$ channels, whose V_{50} was just 2 mV more negative than the human $Ca_v3.1c$ channels [3]. T-type Ca^{2+} channels have been proposed to lead to spontaneous oscillations of the resting membrane potential (reviewed in [12]). To function in this manner, there must be membrane potentials where channels can open but are not completely inactivated. This property has also been called a window current, and is usually defined as the overlap region between the activation and steady-state inactivation curves. Using fits to the data of Fig. 2D, we calculated that 0.2% of channels (percentage of channels activated multiplied by percentage of channels available to activate) may open at −55 mV, and this amount decreases to 0.1% at −50 mV.

The time courses and voltage-dependence of recovery from inactivation, or deinactivation, of human $Ca_v3.1c$ channels were investigated using the voltage protocol illustrated in Fig. 3C. Recovery from inactivation at −100 and −90 mV was basically complete and showed the same time course (time constants of 65 ± 3 and 64 ± 3 ms, respectively). Recovery was incomplete at −80 and −70 mV, and much slower (−80, $\tau=79\pm4$; −70 mV, $\tau=121\pm4$ ms).

The dose-dependence of $NiCl_2$ block was also determined. Nickel produced a fast block that was readily reversed upon washout. Increasing concentrations were assayed without

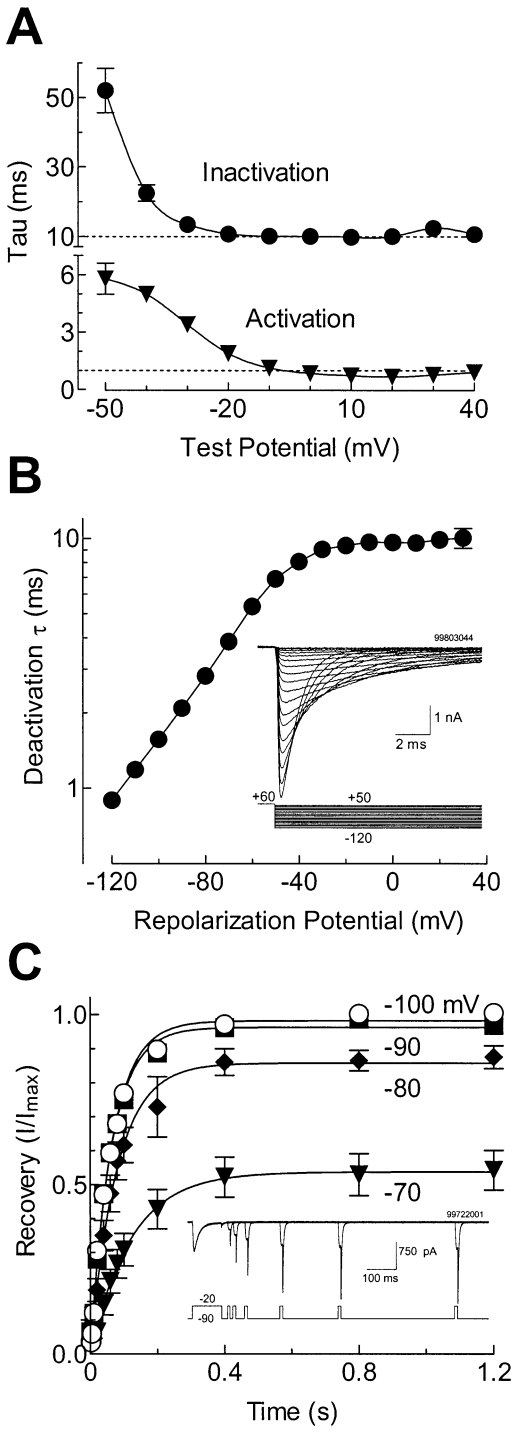

Fig. 3. Kinetic properties of human $Ca_v3.1c$ channels. A: Activation and inactivation tau (τ) values are plotted as a function of test potential. Data points ($n = 16$, in both cases) are the time constants obtained from two exponential fits of currents elicited during the *I-V* protocol (Fig. 2A). B: Voltage-dependence of deactivation kinetics. Tail currents were recorded using the protocol illustrated in the inset. For this cell, the series resistance was 3 MΩ and $C_m = 29$ pF, which produced a clamp speed with a time constant of ~90 μs. The peak of the tail currents was reached at 500 μs. Tail currents were fitted with a simple exponential. Data points show the average of eight cells. C: Time course of recovery from inactivation at different potentials. The inset shows the recovery from inactivation at −90 mV and the two pulse protocol used. Ba^{2+} currents were inactivated by a 100 ms pulse to −20 mV, after which the membrane potential was stepped to −90 mV for periods ranging from 1 to 1200 ms, at which time a 10 ms activating voltage step to −20 mV was applied. The values are the peak current during the 10 ms pulse, divided by the peak current in the 100 ms pulse (I_{max}). The number of cells for each data point varied from seven to 11. Smooth curves are fits to the data using a one phase exponential association equation.

washout as described previously [13]. The IC_{50} was 0.15 ± 0.02 mM ($n = 4$).

4. Discussion

The present study reports the cloning of a novel isoform of α1G from human brain, which we call $Ca_v3.1c$. A full-length cDNA was constructed, then stably-transfected into HEK-293 cells. The resulting channels were analyzed for their time- and voltage-dependent properties.

The CACNA1G gene is alternatively spliced in at least two locations leading to changes in the channel protein. The human isoform reported herein, $Ca_v3.1c$, differs from the one we originally cloned from rat ($Ca_v3.1a$) by having an additional exon, which leads to the addition of 18 amino acids to the linker joining repeats III and IV. The III-IV linker has a number of unusual properties: in both Na^+ and Ca^{2+} channels, it is always much smaller than the linkers joining the other repeats, its sequence is well-conserved within a subfamily (e.g. the T-type subfamily composed of α1G, H and I), and it has been shown to play an important role in the inactivation of Na^+ channels. In fact, a number of human channelopathies are due to mutations in this linker in Na^+ channels (reviewed in [14]). Comparison of the kinetics of the human $Ca_v3.1c$ to those published for the rat $Ca_v3.1a$ [3,11] reveals that the human isoform inactivates and recovers from inactivation ~1.5-fold faster. Although it is tempting to speculate that these differences are due to the III-IV linker splice variation, the contribution of other regions cannot be excluded (see Fig. 1B for location of amino acid substitutions). We have started to address this issue using the rat splice variants, and preliminary results indicate a role of the linker in voltage-dependent gating, but not on the time-dependence of inactivation [6].

The CACNA1G gene contains an unusual splice site between exons 1 and 2, where the splice donor site is CCat and the acceptor is acCT (coding sequence in capitals). A similar AT-AC splice site has been described in a small subset of mammalian genes, including those that encode Na^+ channels [15]. Aberrant splicing of this junction in the Na^+ channel gene, *Scn8a*, leads to the induction of motor endplate disease [16]. It is interesting to speculate that if similar errors occur in the splicing of CACNA1G, they would lead to loss of channel function and decreased neuronal excitability.

The following three properties distinguish T-type channels from high voltage-activated Ca^{2+} channels: activation and inactivation at lower voltages, faster recovery from inactivation, and slower deactivation. These differences may provide insight to their physiological roles. Due to their activation at negative membrane potentials, and because Ca^{2+} entry causes depolarization of the membrane, T-type calcium channels are thought to play an important role as a pacemaker current [17]. For example, in neurons, T-type channels produce the low threshold Ca^{2+} spike that is often crowned by a burst of action potentials mediated by voltage-gated sodium channels

[12]. T-type channels are also thought to play an important role in rebound burst firing, which occurs after inhibitory synaptic potentials (IPSP). The human $Ca_v3.1$ channel has the biophysical properties required to participate in this phenomenon. Specifically, it inactivates over a narrow range of potentials close to the resting membrane potential of many neurons, and unlike HVA channels, it recovers very fast. Both the voltage-dependence and time course of recovery observed with the cloned channel are very similar to the properties observed for the recovery of the low threshold spike in native neurons [18]. The physiological significance of the slow deactivation of T-type channels is unknown. Notably, there appears to be more Ca^{2+} flux through T-type channels after, than during, an action potential [10]. This property may be important for coupling these channels to Ca^{2+}-dependent K^+ channels, which would tend to dampen neuronal excitability [18].

Native T-type currents also differ in their pharmacology. Perhaps the most striking differences noted between T currents from different sources is their sensitivity to nickel [12]. Again, studies on the cloned T-type channels provided a molecular explanation for this heterogeneity, where Ni^{2+} blocks α1H at $\sim$15-fold lower concentrations than either α1G or α1I [13]. The present study shows that Ni^{2+} blocks the human $Ca_v3.1c$ with a similar, albeit slightly higher potency, than its block of the rat $Ca_v3.1a$. We conclude that the sensitivity of native T currents to Ni^{2+} block provides an assay for the expression of α1H.

In conclusion, this study reports the cloning of a full-length sequence of the human α1G and its expression. This sequence information will allow studies aimed at finding mutations, which may underlie neurological disorders. The ability to express the cloned channel at high levels in HEK-293 cells should also allow the development of a high throughput assay for novel drugs.

Acknowledgements: We thank Qun Jiang for technical assistance. This work was supported in part by NIH Grants HL58728 and NS38691. Edward Perez-Reyes is an Established Investigator of the American Heart Association.

References

[1] Perez-Reyes, E. (1999) Cell. Mol. Life Sci. 55, 1–10.
[2] Tsien, R.W. and Tsien, R.Y. (1990) Annu. Rev. Cell Biol. 6, 715–760.
[3] Lee, J.-H., Daud, A.N., Cribbs, L.L., Lacerda, A.E., Pereverzev, A., Klockner, U., Schneider, T. and Perez-Reyes, E. (1999) J. Neurosci. 19, 1912–1921.
[4] Perez-Reyes, E., Cribbs, L.L., Daud, A., Lacerda, A.E., Barclay, J., Williamson, M.P., Fox, M., Rees, M. and Lee, J.-H. (1998) Nature 391, 896–900.
[5] Klugbauer, N., Marais, E., Lacinova, L. and Hofmann, F. (1999) Pflug. Arch. 437, 710–715.
[6] Lee, J.-H., Freihage, J., Cribbs, L.L. and Perez-Reyes, E. (1999) Biophys. J. 76, A408.
[7] Zhuang, H., Hu, F., Bhattacharjee, A., Zhang, M., Wu, S., Berggren, P.-O. and Li, M. (1999) Biophys. J. 76, A409.
[8] Bean, B.P. (1985) J. Gen. Physiol. 86, 1–30.
[9] Chen, C.F. and Hess, P. (1990) J. Gen. Physiol. 96, 603–630.
[10] Randall, A.D. and Tsien, R.W. (1997) Neuropharmacology 36, 879–893.
[11] Serrano, J.R., Perez-Reyes, E. and Jones, S.W. (1999) J. Gen. Physiol. 114, 185–202.
[12] Huguenard, J.R. (1996) Annu. Rev. Physiol. 58, 329–348.
[13] Lee, J.-H., Gomora, J.C., Cribbs, L.L. and Perez-Reyes, E. (1999) Biophys. J. (in press).
[14] Lehmann-Horn, F. and Jurkat-Rott, K. (1999) Physiol. Rev. 79, 1317–1372.
[15] Wu, Q. and Krainer, A.R. (1996) Science 274, 1005–1008.
[16] Kohrman, D.C., Harris, J.B. and Meisler, M. (1996) J. Biol. Chem. 271, 17576–17581.
[17] Ertel, S.I., Ertel, E.A. and Clozel, J.P. (1997) Cardiovasc. Drugs Ther. 11, 723–739.
[18] Aizenman, C.D. and Linden, D.J. (1999) J. Neurophysiol. 82, 1679–1709.